Bounds on Channel Parameter Estimation with 1-bit Quantization and Oversampling

Martin Schlüter, Meik Dörpinghaus, and Gerhard P. Fettweis
Vodafone Chair Mobile Communications Systems, SFB 912 HAEC,
Technische Universität Dresden, Dresden, Germany,
{martin.schlueter, meik.doerpinghaus, gerhard.fettweis}@tu-dresden.de

Abstract—In the design of energy-efficient communication systems with very high bandwidths, the analog-to-digital converter (ADC) plays a crucial role, since its energy consumption grows exponentially with the number of quantization bits. However, high resolution in time domain is less difficult to achieve than high resolution in amplitude domain. This motivates for the design of receivers with 1-bit quantization and oversampling w.r.t. Nyquist rate. On the downside, standard receiver synchronization algorithms cannot be applied, since 1-bit quantization is a highly non-linear function.

To understand the channel parameter estimation performance of such a receiver, the Fisher information (FI) is a helpful measure. Since the closed form evaluation of the FI is not possible for correlated Gaussian noise, we give a lower bound that is an extension of a lower bound by Stein et al. to complex valued channel outputs. If the noise is white, the lower bound is tight. Furthermore, we apply the lower bound for the evaluation of the performance of carrier phase estimation of a QPSK based communication system. We show that for any SNR level oversampling reduces the performance loss due to 1-bit quantization. In the mid and low SNR regime, oversampling reduces the performance loss beyond the loss of $\frac{2}{\pi}$ encountered in case of 1-bit quantization at Nyquist sampling in the low SNR regime.

I. INTRODUCTION

With the increasing demand for faster communication systems, soon data rates of multiple gigabit per second are required. It has recently been understood that analog-to-digital conversion forms a bottleneck at the receiver w.r.t. the power consumption. In particular in wireless short range scenarios, e.g., communication between computer boards [1], [2] an analog-to-digital converter (ADC) with multiple gigasamples per second has a major impact on the overall power consumption of the wireless link. An annually compiled survey on recent advances in ADC design shows that power limited high sampling rates come at the price of coarse quantization [3]. Having this in mind, using an ADC with 1-bit quantization can be beneficial as the low resolution can be compensated by higher sampling rates. It is expected that 1-bit quantization and oversampling is still more energy-efficient than conventional high resolution sampling at Nyquist rate, since neither an automatic gain control, nor linear amplification is required.

Numerical studies have found that sequence design and faster-than-Nyquist (FTN) signaling is beneficial in terms of the achievable rate [4], [5]. Moreover, bounds on the achievable rate of the continuous time (i.e., infinite oversampling) additive white Gaussian noise (AWGN) channel with 1-bit output quantization and strict bandlimitation were derived in [6]. These analytical results confirmed the aforementioned numerical studies.

In [7] the joint synchronization of phase and frequency in a QPSK and Nyquist rate based communication system with coarse quantization was considered. By passing n linear combinations of the in-phase and quadrature components through 1-bit ADCs, phase quantization into $2n$ bins is possible. On the downside, this method increases the energy consumption of the analog-to-digital conversion by factor $\frac{n}{2}$.

However, synchronization under 1-bit quantization and oversampling has not been considered yet. In order to investigate the fundamental limits of the synchronization, one has to analyze the maximum estimation accuracy of parameters (e.g. timing, phase and frequency offset) of the complex channel distribution, which is determined by the Fisher Information (FI) and the Cramér-Rao lower bound (CRLB) [8]. Unfortunately, oversampling w.r.t. Nyquist rate results in noise correlation and it is a mathematically open problem to find an analytical description for the likelihood function of system models with colored Gaussian noise and 1-bit quantization, since there is no analytical description of the orthant probabilities [9]. For real valued signals, Stein et al. derived a lower bound on the FI that requires only the first and second order moments [10]. However, this lower bound is not directly applicable to complex valued signals as they are encountered in the baseband representation of communication systems. We extend this bound to complex valued signals and and show that it is tight in the case of white noise. Furthermore, we apply the lower bound to the problem of carrier phase estimation. While it is known that channel parameter estimation at a receiver with 1-bit quantization and sampling at Nyquist rate shows a performance loss of more than $\frac{2}{\pi}$ compared to the unquantized case [11], [12], we show that oversampling can reduce this performance loss.

II. FISHER INFORMATION LOWER BOUND

Consider the stochastic multivariate system output $\mathbf{r} \in \mathbb{R}^K$ with the likelihood function $p(\mathbf{r}|\boldsymbol{\theta})$ that depends on the deterministic but unknown parameter vector $\boldsymbol{\theta} \in \mathbb{R}^L$. The FI matrix [8, Chapter 3] of the system is defined as

$$[\mathbf{F_r}]_{ij} = \mathrm{E}_{\mathbf{r}|\boldsymbol{\theta}} \left[\left(\frac{\partial \ln p(\mathbf{r}|\boldsymbol{\theta})}{\partial \theta_i} \right) \left(\frac{\partial \ln p(\mathbf{r}|\boldsymbol{\theta})}{\partial \theta_j} \right) \right], \quad (1)$$

with θ_i and θ_j being elements of $\boldsymbol{\theta}$. For any unbiased estimator $\hat{\boldsymbol{\theta}}(\mathbf{r})$, the variance is lower bounded by the CRLB

$$\mathrm{Var} \left[\hat{\theta}_i(\mathbf{r}) \right] \geq \left[\mathbf{F_r}^{-1} \right]_{ii} . \quad (2)$$

For cases where an analytical description of $p(\mathbf{r}|\boldsymbol{\theta})$ is not available or (1) is too difficult to compute, Stein et al. derived a lower bound that requires only the first and second order moments [10]

$$\boldsymbol{\mu}_{\mathbf{r}} = \mathrm{E}\left[\mathbf{r}\right] \tag{3}$$

$$\mathbf{R}_{\mathbf{r}} = \mathrm{E}\left[\mathbf{r}\mathbf{r}^T\right] - \boldsymbol{\mu}_{\mathbf{r}}\boldsymbol{\mu}_{\mathbf{r}}^T \ , \tag{4}$$

which can be computed element-wise. The FI lower bound is given by

$$\mathbf{F}_{\mathbf{r}} \succeq \left(\frac{\partial \boldsymbol{\mu}_{\mathbf{r}}}{\partial \boldsymbol{\theta}}\right)^T \mathbf{R}_{\mathbf{r}}^{-1} \left(\frac{\partial \boldsymbol{\mu}_{\mathbf{r}}}{\partial \boldsymbol{\theta}}\right) = \tilde{\mathbf{F}}_{\mathbf{r}} \tag{5}$$

where $\mathbf{F}_{\mathbf{r}} \succeq \tilde{\mathbf{F}}_{\mathbf{r}}$ denotes that $\mathbf{F}_{\mathbf{r}} - \tilde{\mathbf{F}}_{\mathbf{r}}$ is positive semi-definite. Note that (5) is the exact FI of an unquantized Gaussian system with equal first and second order moment.

Now consider a complex random vector $\mathbf{y} \in \mathbb{C}^K$ with the likelihood function $p(\mathbf{y}|\boldsymbol{\theta})$. The FI matrix and the CRLB are defined as in (1) and (2), respectively. However, the FI lower bound (5) is only valid for real valued random vectors. Thus, we extend the lower bound to complex valued systems by utilizing the FI chain rule [13, Lemma 1]

$$\mathbf{F}_{\mathbf{y}} = \mathbf{F}_{\mathbf{u}} + \mathbf{F}_{\mathbf{v}|\mathbf{u}}, \tag{6}$$

with $\mathbf{y} = \mathbf{u} + j\mathbf{v}$ and

$$\left[\mathbf{F}_{\mathbf{v}|\mathbf{u}}\right]_{ij} = \mathrm{E}_{\mathbf{u},\mathbf{v}|\boldsymbol{\theta}}\left[\left(\frac{\partial \ln p(\mathbf{v}|\mathbf{u},\boldsymbol{\theta})}{\partial \theta_i}\right)\left(\frac{\partial \ln p(\mathbf{v}|\mathbf{u},\boldsymbol{\theta})}{\partial \theta_j}\right)\right]. \tag{7}$$

We now have decomposed the FI into two parts that only depend on real random vectors and, thus, we can apply the lower bound (5), such that

$$\mathbf{F}_{\mathbf{y}} \succeq \tilde{\mathbf{F}}_{\mathbf{u}} + \tilde{\mathbf{F}}_{\mathbf{v}|\mathbf{u}} = \tilde{\mathbf{F}}_{\mathbf{y}} \ . \tag{8}$$

If $\mathbf{u}$ and $\mathbf{v}$ are independent, (6) and (8) reduce to

$$\mathbf{F}_{\mathbf{y}} = \mathbf{F}_{\mathbf{u}} + \mathbf{F}_{\mathbf{v}} \succeq \tilde{\mathbf{F}}_{\mathbf{u}} + \tilde{\mathbf{F}}_{\mathbf{v}} = \tilde{\mathbf{F}}_{\mathbf{y}} \ . \tag{9}$$

III. CHANNEL PARAMETER ESTIMATION WITH 1-BIT QUANTIZATION AND COLORED GAUSSIAN NOISE

We assume a complex-valued observation vector

$$\begin{aligned}
\mathbf{y} &= \mathrm{csign}\left(\mathbf{s}(\boldsymbol{\theta}) + \boldsymbol{\eta}\right) \\
&= \mathrm{sign}\left(\mathrm{Re}\left\{\mathbf{s}(\boldsymbol{\theta}) + \boldsymbol{\eta}\right\}\right) + j \cdot \mathrm{sign}\left(\mathrm{Im}\left\{\mathbf{s}(\boldsymbol{\theta}) + \boldsymbol{\eta}\right\}\right) \\
&= \mathbf{u} + j\mathbf{v},
\end{aligned} \tag{10}$$

with the signum function

$$\mathrm{sign}\left(x\right) = \begin{cases} 1 & x > 0 \\ -1 & x \leq 0 \end{cases} \tag{11}$$

that is applied elementwise. The vector $\mathbf{s}(\boldsymbol{\theta}) \in \mathbb{C}^K$ contains the information on the transmitted data altered by the channel that is characterized by the deterministic but unknown parameter vector $\boldsymbol{\theta} \in \mathbb{R}^L$. The vector $\boldsymbol{\eta} \sim \mathcal{CN}\left(0, \mathbf{R}_{\boldsymbol{\eta}}\right)$ is a circularly-symmetric complex Gaussian random vector with independent real and imaginary part. Furthermore, $\mathbf{s}(\boldsymbol{\theta})$ and $\boldsymbol{\eta}$ are independent.

Unfortunately, a compact analytical description of the likelihood function $p(\mathbf{y}|\mathbf{s}(\boldsymbol{\theta}))$ is only available in the case of white noise, i.e., $\mathbf{R}_{\boldsymbol{\eta}} = \sigma^2 \mathbf{I}$, where $\mathbf{I}$ is the identity matrix. It is a mathematically open problem to find an analytical description for the likelihood function of system models with colored Gaussian noise and 1-bit quantization, since there is no analytical description of the orthant probabilities [9]. However, we can apply (9) to lower bound the FI.

Since the lower-bounding technique is identical for both, the real and the imaginary part, we present only the derivation of $\tilde{\mathbf{F}}_{\mathbf{u}}$. The mean value of $\mathbf{u}$ is given by

$$\begin{aligned}
\left[\boldsymbol{\mu}_{\mathbf{u}}\right]_k &= p\left(u_k = +1|\mathbf{s}(\boldsymbol{\theta})\right) - p\left(u_k = -1|\mathbf{s}(\boldsymbol{\theta})\right) \\
&= 1 - 2Q\left(\frac{\mathrm{Re}\left\{s_k(\boldsymbol{\theta})\right\}}{\sqrt{\left[\mathbf{R}_{\boldsymbol{\eta}}\right]_{kk}/2}}\right) ,
\end{aligned} \tag{12}$$

where $Q(\cdot)$ denotes the Q-function

$$Q(x) = \frac{1}{\sqrt{2\pi}} \int_x^\infty \exp\left(-\frac{u^2}{2}\right) du \ . \tag{13}$$

The derivative of (12) is given by

$$\frac{\partial \left[\boldsymbol{\mu}_{\mathbf{u}}\right]_k}{\partial \theta_i} = \frac{2 \exp\left\{-\frac{\mathrm{Re}\left\{s_k(\boldsymbol{\theta})\right\}^2}{\left[\mathbf{R}_{\boldsymbol{\eta}}\right]_{kk}}\right\} \frac{\partial}{\partial \theta_i} \mathrm{Re}\left\{s_k(\boldsymbol{\theta})\right\}}{\sqrt{\pi \left[\mathbf{R}_{\boldsymbol{\eta}}\right]_{kk}}} . \tag{14}$$

The diagonal elements of the covariance matrix are given by

$$\left[\mathbf{R}_{\mathbf{u}}\right]_{kk} = 1 - \left[\boldsymbol{\mu}_{\mathbf{u}}\right]_k^2 \ , \tag{15}$$

while the off-diagonal elements are calculated as

$$\begin{aligned}
\left[\mathbf{R}_{\mathbf{u}}\right]_{kn} = 2 &\left[p\left(z_k > 0, z_n > 0\right) + p\left(z_k \leq 0, z_n \leq 0\right)\right] \\
&- 1 - \left[\boldsymbol{\mu}_{\mathbf{u}}\right]_k \left[\boldsymbol{\mu}_{\mathbf{u}}\right]_n
\end{aligned} \tag{16}$$

where $\left[z_k, z_n\right]^T$ is a bi-variate Gaussian random vector

$$\begin{bmatrix} z_k \\ z_n \end{bmatrix} \sim \mathcal{N}\left(\begin{bmatrix} \mathrm{Re}\left\{s_k(\boldsymbol{\theta})\right\} \\ \mathrm{Re}\left\{s_n(\boldsymbol{\theta})\right\} \end{bmatrix}, \frac{1}{2}\begin{bmatrix} \left[\mathbf{R}_{\boldsymbol{\eta}}\right]_{kk} & \left[\mathbf{R}_{\boldsymbol{\eta}}\right]_{kn} \\ \left[\mathbf{R}_{\boldsymbol{\eta}}\right]_{nk} & \left[\mathbf{R}_{\boldsymbol{\eta}}\right]_{nn} \end{bmatrix}\right). \tag{17}$$

Thus, (16) can only be obtained numerically. The lower bound for the imaginary part of $\mathbf{y}$ is derived in the same manner.

IV. CHANNEL PARAMETER ESTIMATION WITH 1-BIT QUANTIZATION AND WHITE GAUSSIAN NOISE

Consider the system model (10), but now the noise is white, i.e., $\mathbf{R}_{\boldsymbol{\eta}} = \sigma^2 \mathbf{I}$. In this case, it is possible to describe the likelihood function in an analytical form and, thus, it is possible to derive the FI. Since the elements y_k and y_n of $\mathbf{y}$ are independent conditioned on $\mathbf{s}(\boldsymbol{\theta})$ if $k \neq n$, the likelihood function is given by

$$\begin{aligned}
p\left(\mathbf{y}|\mathbf{s}(\boldsymbol{\theta})\right) &= \prod_{k=1}^K p\left(y_k|s_k(\boldsymbol{\theta})\right) \\
&= \prod_{k=1}^K p\left(u_k|s_k(\boldsymbol{\theta})\right) p\left(v_k|s_k(\boldsymbol{\theta})\right),
\end{aligned} \tag{18}$$

with

$$p\left(u_k = +1|s_k(\boldsymbol{\theta})\right) = Q\left(-\frac{\mathrm{Re}\left\{s_k(\boldsymbol{\theta})\right\}}{\sigma/\sqrt{2}}\right) \tag{19}$$

and

$$p\left(u_k = -1 | s_k\left(\boldsymbol{\theta}\right)\right) = Q\left(\frac{\mathrm{Re}\left\{s_k(\boldsymbol{\theta})\right\}}{\sigma/\sqrt{2}}\right). \qquad (20)$$

The probability $p\left(v_k | s_k\left(\boldsymbol{\theta}\right)\right)$ is defined in the same manner, such that

$$p(\mathbf{y}|\mathbf{s}(\boldsymbol{\theta})) = \prod_{k=1}^{K} Q\left(-u_k \frac{\mathrm{Re}\{s_k(\boldsymbol{\theta})\}}{\sigma/\sqrt{2}}\right) Q\left(-v_k \frac{\mathrm{Im}\{s_k(\boldsymbol{\theta})\}}{\sigma/\sqrt{2}}\right). \qquad (21)$$

To derive the FI, we apply the FI chain rule, such that using the independency of $\mathbf{u} = [u_1, u_2, \cdots, u_K]$ and $\mathbf{v} = [v_1, v_2, \cdots, v_K]$ results in

$$\mathbf{F}_{\mathbf{y}} = \sum_{k=1}^{K} \left(\mathbf{F}_{u_k} + \mathbf{F}_{v_k}\right). \qquad (22)$$

We again restrict the presentation to the FI of the real part, since the derivation for the imaginary part is analogous. With

$$\frac{d}{dx} \ln Q\left(f(x)\right) = -\frac{\exp\left\{-f^2(x)/2\right\} \frac{d}{dx} f(x)}{\sqrt{2\pi} Q\left(f(x)\right)} \qquad (23)$$

the FI of u_k is given by

$$[\mathbf{F}_{u_k}]_{ij} = \frac{1}{\pi \sigma^2}$$
$$\times \mathrm{E}_{u_k | s_k(\theta)} \left[\frac{\exp\left\{-\frac{\mathrm{Re}\{s_k(\boldsymbol{\theta})\}^2}{\sigma^2/2}\right\} \frac{\partial}{\partial \theta_i} \mathrm{Re}\{s_k(\boldsymbol{\theta})\} \frac{\partial}{\partial \theta_j} \mathrm{Re}\{s_k(\boldsymbol{\theta})\}}{Q\left(-u_k \frac{\mathrm{Re}\{s_k(\boldsymbol{\theta})\}}{\sigma/\sqrt{2}}\right)^2} \right]. \qquad (24)$$

We utilize (19) and (20) to evaluate the expected value, such that

$$[\mathbf{F}_{u_k}]_{ij} = \frac{1}{\pi \sigma^2}$$
$$\times \frac{\exp\left\{-\frac{\mathrm{Re}\{s_k(\boldsymbol{\theta})\}^2}{\sigma^2/2}\right\} \frac{\partial}{\partial \theta_i} \mathrm{Re}\{s_k(\boldsymbol{\theta})\} \frac{\partial}{\partial \theta_j} \mathrm{Re}\{s_k(\boldsymbol{\theta})\}}{Q\left(\frac{\mathrm{Re}\{s_k(\boldsymbol{\theta})\}}{\sigma/\sqrt{2}}\right) Q\left(-\frac{\mathrm{Re}\{s_k(\boldsymbol{\theta})\}}{\sigma/\sqrt{2}}\right)} \qquad (25)$$

and finally

$$[\mathbf{F}_{\mathbf{y}}]_{ij} = \frac{1}{\pi \sigma^2}$$
$$\times \sum_{k=1}^{K} \left(\frac{\exp\left\{-\frac{\mathrm{Re}\{s_k(\boldsymbol{\theta})\}^2}{\sigma^2/2}\right\} \frac{\partial}{\partial \theta_i} \mathrm{Re}\{s_k(\boldsymbol{\theta})\} \frac{\partial}{\partial \theta_j} \mathrm{Re}\{s_k(\boldsymbol{\theta})\}}{Q\left(\frac{\mathrm{Re}\{s_k(\boldsymbol{\theta})\}}{\sigma/\sqrt{2}}\right) Q\left(-\frac{\mathrm{Re}\{s_k(\boldsymbol{\theta})\}}{\sigma/\sqrt{2}}\right)} \right.$$
$$\left. + \frac{\exp\left\{-\frac{\mathrm{Im}\{s_k(\boldsymbol{\theta})\}^2}{\sigma^2/2}\right\} \frac{\partial}{\partial \theta_i} \mathrm{Im}\{s_k(\boldsymbol{\theta})\} \frac{\partial}{\partial \theta_j} \mathrm{Im}\{s_k(\boldsymbol{\theta})\}}{Q\left(\frac{\mathrm{Im}\{s_k(\boldsymbol{\theta})\}}{\sigma/\sqrt{2}}\right) Q\left(-\frac{\mathrm{Im}\{s_k(\boldsymbol{\theta})\}}{\sigma/\sqrt{2}}\right)} \right). \qquad (26)$$

Let us now derive the FI lower bound for the case of white noise. As the off-diagonal elements of $\mathbf{R}_{\boldsymbol{\eta}}$ are zero, the off-diagonal elements of $\mathbf{R}_{\mathbf{u}}$ and $\mathbf{R}_{\mathbf{v}}$ are also zero. Hence, (5) reduces to

$$\left[\tilde{\mathbf{F}}_{\mathbf{u}}\right]_{ij} = \sum_{k=1}^{K} \frac{\partial \left[\boldsymbol{\mu}_{\mathbf{u}}\right]_k}{\partial \theta_i} \frac{\partial \left[\boldsymbol{\mu}_{\mathbf{u}}\right]_k}{\partial \theta_j} \frac{1}{\left[\mathbf{R}_{\mathbf{u}}\right]_{kk}}, \qquad (27)$$

with

$$[\mathbf{R}_{\mathbf{u}}]_{kk} = 1 - [\boldsymbol{\mu}_{\mathbf{u}}]_k^2$$
$$= 1 - \left(1 - 2Q\left(\frac{\mathrm{Re}\{s_k(\boldsymbol{\theta})\}}{\sigma/\sqrt{2}}\right)\right)^2 \qquad (28)$$
$$= 4Q\left(\frac{\mathrm{Re}\{s_k(\boldsymbol{\theta})\}}{\sigma/\sqrt{2}}\right) Q\left(-\frac{\mathrm{Re}\{s_k(\boldsymbol{\theta})\}}{\sigma/\sqrt{2}}\right)$$

and $\frac{\partial [\boldsymbol{\mu}_{\mathbf{u}}]_k}{\partial \theta_i}$ given in (14) such that

$$\left[\tilde{\mathbf{F}}_{\mathbf{u}}\right]_{ij} = \frac{1}{\pi \sigma^2}$$
$$\times \sum_{k=1}^{K} \frac{\exp\left\{-\frac{\mathrm{Re}\{s_k(\boldsymbol{\theta})\}^2}{\sigma^2/2}\right\} \frac{\partial}{\partial \theta_i} \mathrm{Re}\{s_k(\boldsymbol{\theta})\} \frac{\partial}{\partial \theta_j} \mathrm{Re}\{s_k(\boldsymbol{\theta})\}}{Q\left(\frac{\mathrm{Re}\{s_k(\boldsymbol{\theta})\}}{\sigma/\sqrt{2}}\right) Q\left(-\frac{\mathrm{Re}\{s_k(\boldsymbol{\theta})\}}{\sigma/\sqrt{2}}\right)}. \qquad (29)$$

Since $\tilde{\mathbf{F}}_{\mathbf{v}}$ is obtained in the same manner, we see that for white noise the FI lower bound equals the actual FI of the system in (26), i.e., $\mathbf{F}_{\mathbf{y}} = \tilde{\mathbf{F}}_{\mathbf{y}}$. This serves as a motivation to use the lower bound in the case of colored noise, where a closed form solution of the exact FI is not available.

V. APPLICATION: CARRIER PHASE ESTIMATION

We now apply the FI lower bound to the problem of estimating the carrier phase offset in a QPSK signal with M transmit symbols under 1-bit quantization and oversampling. We consider the complex valued receive signal

$$r(t) = \sum_{m=1}^{M} a_m g(t - mT) e^{j\phi} + \eta(t) \qquad (30)$$

with deterministic but unknown phase rotation ϕ and ideal rectangular transmit and receive filters with single sided bandwidth $W = \frac{1}{2T}$. That means that $g(t)$ is a sinc pulse and the power spectral density (PSD) of the Gaussian noise $\eta(t)$ is given by

$$S_\eta(f) = \frac{N_0}{2} \mathrm{rect}\left(\frac{f}{2W}\right) \qquad (31)$$

where $\mathrm{rect}\left(\cdot\right)$ is the rectangular function. Thus, according to the Wiener-Khinchin theorem $\eta(t)$ has the auto-correlation function

$$r_\eta(\tau) = W N_0 \mathrm{sinc}\left(2W\tau\right). \qquad (32)$$

Furthermore, we assume the QPSK constellation $a_m \in \left\{e^{j\frac{\pi}{4}}, e^{j\frac{3}{4}\pi}, e^{j\frac{5}{4}\pi}, e^{j\frac{7}{4}\pi}\right\}$. The analog receive signal $r(t)$ is sampled with an oversampling factor M_{os} such that after 1-bit quantization we get

$$y_k = \mathrm{csign}\left(\sum_{m=1}^{M} a_m g\left(k\frac{T}{M_{\mathrm{os}}} - mT\right) e^{j\phi} + \eta\left(k\frac{T}{M_{\mathrm{os}}}\right)\right) \qquad (33)$$

and the noise covariance matrix of dimension $M M_{\mathrm{os}} \times M M_{\mathrm{os}}$ is given by

$$[\mathbf{R}_{\boldsymbol{\eta}}]_{kn} = W N_0 \mathrm{sinc}\left(2W \frac{T}{M_{\mathrm{os}}}|n - k|\right)$$
$$= \sigma^2 \mathrm{sinc}\left(\frac{1}{M_{\mathrm{os}}}|n - k|\right). \qquad (34)$$
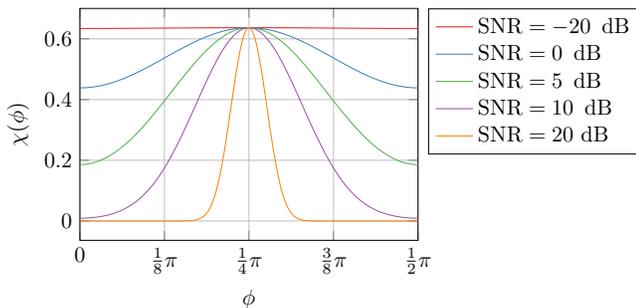
Fig. 1. FI ratio $\chi(\phi)$ for $M = 1$ and $M_{\text{os}} = 1$

Fig. 2. $\mathrm{E}_{\phi,\mathbf{a}}\left[\chi(\phi)\right]$ for $M = 10$ random but known QPSK symbols

One observes that only for $M_{\text{os}} = 1$, i.e., sampling at Nyquist rate, the noise is white with $\mathbf{R}_{\boldsymbol{\eta}} = \sigma^2\mathbf{I}$.

As a benchmark for the receiver based on 1-bit quantization and oversampling, we use a receiver based on unquantized Nyquist sampling, i.e., the receiver has access to the signal

$$z_k = \sum_{m=1}^{M} a_m g\left(kT - mT\right) e^{j\phi} + \eta(kT). \tag{35}$$

The FI of the phase ϕ of this signal model is known to be [14, p. 337]

$$F_{\mathbf{z}}(\phi) = 2M\frac{E_s}{\sigma^2} \tag{36}$$

where E_s is the symbol energy and, thus, E_s/σ^2 is the SNR. The performance gap between the unquantized receiver (35) and the 1-bit receiver (33) with respect to the estimation of ϕ can be lower bounded by the ratio

$$\chi(\phi) = \frac{\tilde{F}_{\mathbf{y}}(\phi)}{F_{\mathbf{z}}(\phi)} \tag{37}$$

where $\tilde{F}_{\mathbf{y}}(\phi)$ is the FI lower bound of ϕ based on $\mathbf{y}$. For the low SNR limit, it is known that for any parameter θ, without oversampling the ratio $\chi(\theta)$ converges to $\lim_{\sigma \to \infty} \chi(\theta) = \frac{2}{\pi}$.

We start with investigating the problem of estimating ϕ under the assumption of a single observation, i.e., $M = 1$ and $M_{\text{os}} = 1$. For this case, the FI can be computed exactly with (26), i.e., $F_{\mathbf{y}}(\phi) = \tilde{F}_{\mathbf{y}}(\phi)$ and (37) is the exact characterization of the performance loss. Fig. 1 depicts $\chi(\phi)$ for different SNR values and ϕ in the range $\left[0, \frac{\pi}{2}\right]$, as $F_{\mathbf{y}}(\phi)$ is periodic with period $\frac{\pi}{2}$. Thus, $F_{\mathbf{y}}(\phi)$ is independent of the data symbol since all QPSK symbols modulo $\frac{\pi}{2}$ have the same phase. Note that the dependency of $\chi(\phi)$ on ϕ is only due to $F_{\mathbf{y}}(\phi)$ as $F_{\mathbf{z}}(\phi)$ is independent of ϕ. We observe that for low SNR $\chi(\phi)$ is almost flat and for high SNR it has a maximum around $\phi = \frac{\pi}{4}$, i.e., the phase rotation that brings the QPSK symbol to the decision boundary. This is intuitive, since at high SNR in every symbol period the same measurement would be observed if the QPSK symbol would be in the middle of a quadrant, which results in a poor estimate of ϕ. As the SNR decreases, the noise leads to a more uniform distribution of the received phase on the unit circle and the FI becomes less dependent on the phase rotation ϕ. Moreover, we observe that regardless of the SNR, $\chi(\phi)$ never exceeds the limit $\frac{2}{\pi}$.

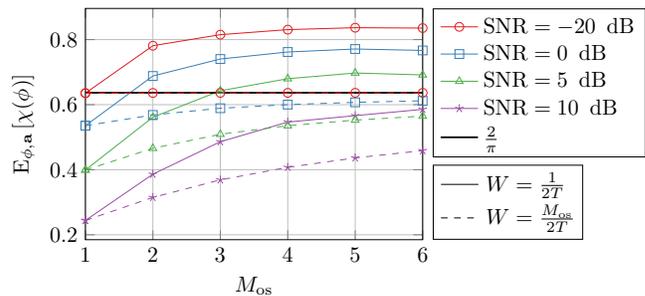Let us now investigate the effect of the oversampling factor M_{os} under the assumption of $M = 10$ independent and equally likely random but known transmit symbols. Since $\tilde{F}_{\mathbf{y}}(\phi)$ depends on the phase rotation ϕ, we investigate the expected value w.r.t. ϕ. Moreover, due to oversampling $\tilde{F}_{\mathbf{y}}(\phi)$ also depends on the transmit symbols a_m, since between the transmit symbols the transmit signal depends on the actual transmit symbol sequence and the shape of the transmit pulse. Since finding an optimal pilot sequence is not in the focus of the present work, the solid lines in Fig. 2 plot $\mathrm{E}_{\phi,\mathbf{a}}\left[\chi(\phi)\right]$ against M_{os}, where we assumed ϕ is uniformly distributed on the interval $[0, 2\pi)$. We observe that for low SNR and $M_{\text{os}} = 1$ the classical result of $\frac{2}{\pi}$ is attained and for higher SNR the performance loss is increasing. However, with increasing oversampling factor the performance loss is decreasing and the $\frac{2}{\pi}$ limit for Nyquist sampling can be surpassed. In [15], similar observations were made for the time-of-arrival estimation in a GPS like setup. Moreover, with an increasing oversampling factor the curves are saturating due to noise correlation. The higher M_{os} the more pronounced is the noise correlation, see (34). Furthermore, oversampling only increases the accuracy of the knowledge on the zero crossings of the signal. Information that is only contained inside the amplitude cannot be recovered by oversampling.

In comparison to the case of colored noise, the dashed lines in Fig. 2 show the FI ratio for the case that we adapt the filter bandwidth to the oversampling factor, i.e., $W = \frac{M_{\text{os}}}{2T}$. As can be seen in (34), this yields white noise but increases the noise power by M_{os}. Thus, the curves converge to $\frac{2}{\pi}$ as $M_{\text{os}} \to \infty$.

VI. CONCLUSION

We extended a known lower bound for the FI of real valued observations to complex valued observations. The bound was applied to the general problem of signal parameter estimation with 1-bit quantization and circularly-symmetric complex Gaussian noise. For the case of white noise, the FI can be computed exactly and is equal to the lower bound, which shows its applicability. We further applied the bound to the problem of carrier phase estimation in a wireless communication receiver with 1-bit quantization and oversampling. We observe that oversampling decreases the performance loss w.r.t. to the unquantized system with Nyquist sampling beyond the known low SNR limit of $\frac{2}{\pi}$.

REFERENCES

[1] G. Fettweis, N. ul Hassan, L. Landau, and E. Fischer, "Wireless interconnect for board and chip level," in *Proc. IEEE Des. Autom. Test Eur. Conf. Exhib.*, Grenoble, France, May 2013, pp. 958–963.

[2] M. Jenning, B. Klein, R. Hahnel, D. Plettemeier, D. Fritsche, G. Tretter, C. Carta, F. Ellinger, T. Nardmann, M. Schroter, K. Nieweglowski, K. Bock, J. Israel, A. Fischer, N. Ul Hassan, L. Landau, M. Dörpinghaus, and G. Fettweis, "Energy-efficient transceivers for ultra-highspeed computer board-to-board communication," in *Proc. IEEE Int. Conf. Ubiquitous Wirel. Broadband*, Montreal, Canada, Oct. 2015, pp. 1–5.

[3] B. Murmann, "ADC performance survey 1997-2017." [Online]. Available: http://web.stanford.edu/ murmann/adcsurvey.html

[4] L. Landau, M. Dörpinghaus, and G. Fettweis, "Communications employing 1-bit quantization and oversampling at the receiver: Faster-than-Nyquist signaling and sequence design," in *Proc. IEEE Int. Conf. Ubiquitous Wirel. Broadband*, Montreal, Canada, Oct. 2015.

[5] ——, "1-bit quantization and oversampling at the receiver: Communication over bandlimited channels with noise," *IEEE Commun. Lett.*, vol. 21, no. 5, pp. 1007–1010, May 2017.

[6] S. Bender, M. Dörpinghaus, and G. Fettweis, "On the achievable rate of bandlimited continuous-time 1-bit quantized AWGN channels," in *Proc. IEEE Int. Symp. Inf. Theory*, Aachen, Germany, Jun. 2017, pp. 2083–2087.

[7] A. Wadhwa and U. Madhow, "Near-coherent QPSK performance with coarse phase quantization: A feedback-based architecture for joint phase/frequency synchronization and demodulation," *IEEE Trans. Signal Process.*, vol. 64, no. 17, pp. 4432–4443, Sep. 2016.

[8] S. M. Kay, *Fundamentals of Statistical Signal Processing: Estimation Theory.* Upper Saddle River, NJ, USA: Prentice-Hall, Inc., 1993.

[9] A. Genz and F. Bretz, *Computation of Multivariate Normal and t Probabilities*, 1st ed. Berlin Heidelberg: Springer, 2009.

[10] M. Stein, A. Mezghani, and J. A. Nossek, "A lower bound for the Fisher information measure," *IEEE Signal Process. Lett.*, vol. 21, no. 7, pp. 796–799, Jul. 2014.

[11] M. Stein, A. Kurzl, A. Mezghani, and J. A. Nossek, "Asymptotic parameter tracking performance with measurement data of 1-bit resolution," *IEEE Trans. Signal Process.*, vol. 63, no. 22, pp. 6086–6095, Nov. 2015.

[12] G. Zeitler, G. Kramer, and A. C. Singer, "Bayesian parameter estimation using single-bit dithered quantization," *IEEE Trans. Signal Process.*, vol. 60, no. 6, pp. 2713–2726, Jun. 2012.

[13] R. Zamir, "A proof of the Fisher information inequality via a data processing argument," *IEEE Trans. Inf. Theory*, vol. 44, no. 3, pp. 1246–1250, May 1998.

[14] H. Meyr, M. Moeneclaey, and S. Fechtel, *Digital Communication Receivers: Synchronization, Channel Estimation, and Signal Processing.* New York, NY, USA: John Wiley & Sons, Inc., 1997.

[15] M. Stein, "Performance analysis for time-of-arrival estimation with oversampled low-complexity 1-bit a/d conversion," in *Proc. IEEE Int. Conf. Acoust. Speech Signal Process.*, New Orleans, USA, Mar. 2017, pp. 4491–4495.